Electronic Structure of Zirconium*

T. L. Loucks†
Institute for Atomic Research and Department of Physics, Iowa State University, Ames, Iowa
(Received 19 December 1966)

Augmented-plane-wave (APW) calculations of the electronic structure of zirconium have been carried out. The resulting Fermi surface is almost entirely different from the model proposed earlier by Altmann and Bradley on the basis of cellular calculations. The APW Fermi surface (after slight modification) can account for the angular dependence of the de Haas–van Alphen periods observed by Thorsen and Joseph; the theoretical values of the periods differ from the experimental results by no more than about 40%. Although this is by no means an outstanding example of close agreement between experimental and theoretical results, it is believed that the new Fermi-surface model represents a substantial improvement over previous work and is a better starting point for any future attempts to deduce an improved model whenever additional experimental data become available.

INTRODUCTION

ZIRCONIUM is a transiton metal (atomic configuration $4d^25s^2$) which crystallizes in the hexagonal close-packed (hcp) structure. The only experimental results relating directly to the Fermi surface of this metal are the de Haas-van Alphen (dHvA) measurements of Thorsen and Joseph(TJ).[1] Their results are extremely complicated and cannot be explained in terms of the nearly-free-electron model. The only theoretical calculation of the Fermi surface of zirconium has been presented by Altmann and Bradley[2] (AB), who used the form of the cellular method suggested by Slater.[3] The resulting Fermi surface, it is claimed by these authors, can account (at least approximately) for the angular dependence of four out of the five periods reported by TJ. This being the case, theirs was the first such calculation showing an agreement of this type for a transition metal.[4–6]

Since that time there have been several energy-band calculations for transition metals, many of these based on the augmented-plane-wave (APW) method originated and developed by Slater.[7] This method has been used successfully in many applications, not only for transition elements, but also for simple metals, compounds, and ionic crystals.[8] An example of the accuracy that can be expected from this method can be found in the good agreement between experimental results and the theoretical Fermi surfaces of Mo and W.[9–11] Another good example, in this case for an hcp transition metal, is the APW calculation for rhenium given by Mattheiss.[12] Other Fermi-surface calculations for hcp transition metals have been performed using the APW method,[13–17] but lack of experimental data precludes a direct check of these results at the present time.

However, it can be observed that in the APW calculations for hcp transition metals, in particular for Re,[12] Gd,[13] Y,[16] and Dy,[17] the density-of-states curves are all strikingly similar. There are, of course, small variations in the energy bands for the different metals, but the general features of the curves are all very much the same. In particular, for all of these metals the energy corresponding to four electrons per atom (as in Zr) occurs near a sharp minimum in the density of states (actually up slightly on the high-energy side). This minimum separates two large peaks resulting from the contributions of the relatively narrow d bands.

The cellular calculations by AB,[18] however, do not exhibit this characteristic in the density of states curve. The general features of their curve are different, and the Fermi energy occurs on a relatively high, wide, and nearly flat portion of the curve. This apparent discrepancy catalyzed the author's latent distrust of the cellular method and led him to examine more carefully the corresponding Fermi-surface model of AB.[2] Certain ambiguities were found. For instance, there are two dHvA periods (designated α and β by TJ) which have their minimum separation (about 10%) for the field direction along the c axis. As the field is tilted away

* Work was performed in the Ames Laboratory of the U. S. Atomic Energy Commission. Contribution No. 2004.
† Alfred P. Sloan Research Fellow.
[1] A. C. Thorsen and A. S. Joseph, Phys. Rev. **131**, 2078 (1963).
[2] S. L. Altmann and C. J. Bradley, Phys. Rev. **135**, A1253 (1964).
[3] J. C. Slater, Phys. Rev. **45**, 794 (1934).
[4] Actually the first such calculation was that of Burdick [see Refs. 5 and 6] for copper, but since the d bands are beneath the Fermi energy in this metal, the Fermi surface is very simple and can be described by the nearly-free-electron model.
[5] G. A. Burdick, Phys. Rev. Letters **7**, 156 (1961).
[6] G. A. Burdick, Phys. Rev. **129**, 138 (1963).
[7] J. C. Slater, Phys. Rev. **51**, 846 (1937).
[8] For a review of earlier work see J. C. Slater, *Advances in Quantum Chemistry* (Academic Press Inc., New York, 1964), Vol. 1, p. 35; J. C. Slater, *Quantum Theory of Molecules and Solids* (McGraw-Hill Book Company, Inc., New York, 1965), Vol. 2. For a more recent summary of APW calculations, along with a detailed description of both the theoretical and practical aspects of this method, see T. L. Loucks, *Augmented Plane Wave Method* (W. A. Benjamin, Inc., New York, 1967).
[9] T. L. Loucks, Phys. Rev. **139**, A1181 (1965).
[10] L. F. Mattheiss, Phys. Rev. **139**, A1893 (1965).
[11] T. L. Loucks, Phys. Rev. **143**, 506 (1966).
[12] L. F. Mattheiss, Phys. Rev. **151**, 450 (1966).
[13] J. O. Dimmock and A. J. Freeman, Phys. Rev. Letters **13**, 750 (1964).
[14] A. J. Freeman, J. O. Dimmock, and R. E. Watson, Phys. Rev. Letters **16**, 94 (1966).
[15] R. W. Williams, T. L. Loucks, and A. R. Mackintosh, Phys. Rev. Letters **16**, 168 (1966).
[16] T. L. Loucks, Phys. Rev. **144**, 504 (1966).
[17] S. C. Keeton, Ph.D. thesis, Iowa State University, Ames, Iowa, 1966 (unpublished).
[18] S. L. Altmann and C. J. Bradley, Phys. Letters **1**, 336 (1936).

TABLE I. Muffin-tin potential for zirconium inside APW spheres.

$\ln r$	$-r^2V(r)$	$\ln r$	$-r^2V(r)$	$\ln r$	$-r^2V(r)$
−2.85	3.643	−1.55	8.272	−0.25	9.842
−2.75	3.938	−1.45	8.611	−0.15	9.665
−2.65	4.249	−1.35	8.930	−0.05	9.440
−2.55	4.576	−1.25	9.220	0.05	9.138
−2.45	4.918	−1.15	9.476	0.15	8.729
−2.35	5.273	−1.05	9.691	0.25	8.198
−2.25	5.640	−0.95	9.864	0.35	7.537
−2.15	6.016	−0.85	9.996	0.45	6.744
−2.05	6.398	−0.75	10.09	0.55	5.824
−1.95	6.783	−0.65	10.14	0.65	4.789
−1.85	7.168	−0.55	10.14	0.75	3.673
−1.75	7.547	−0.45	10.09	0.85	2.532
−1.65	7.916	−0.35	9.986	0.95	1.437
				1.05	0.479

from the c axis, the smaller period decreases and the larger one increases. AB have assigned these periods to a dumbbell-shaped piece of Fermi surface with its symmetry axis along the c direction. For such a surface the periods corresponding to the maximum and minimum orbits would come together at some angle rather than separating further (as is actually observed experimentally).

[*Note added in proof.* Since this article was written the author has had the pleasure of discussing the work with Professor S. L. Altmann at Oxford University. From his unpublished results (some of which have been presented at conferences in the form of slides), it appears that the differences in our results are primarily due to the potentials used rather than to any inherent difficulties in the form of the cellular method. More is said about this in the Discussion.]

It was decided to calculate the energy bands and Fermi surface of Zr using the APW method to see if these ambiguities could at least be partially resolved. As expected, the resulting density-of-states curve was found to have the same general features as all of the other APW calculations for hcp transition metals. The value of the density of states at the Fermi energy is consistent with the value obtained from the experimental electronic specific-heat coefficient (approximately the same electron-phonon enhancement factor being required as for neighboring yttrium and the hcp rare-earth metals). The APW Fermi surface is almost completely different from the one proposed by AB, but it accounts semiqualitatively for all the dHvA periods

TABLE II. The 32 reciprocal lattice vectors used in the APW expansion.

	$(2\bar{1}1)$	$(2\bar{1}0)$	(200)				
$(10\bar{1})$	$(1\bar{1}1)$	$(1\bar{1}0)$	(100)	(110)	$(11\bar{1})$	(101)	$(1\bar{2}1)$
$(00\bar{1})$	$(0\bar{1}1)$	$(0\bar{1}0)$	(000)	(010)	$(01\bar{1})$	(001)	$(0\bar{2}1)$
$(\bar{1}0\bar{1})$	$(\bar{1}\bar{1}1)$	$(\bar{1}\bar{1}0)$	$(\bar{1}00)$	$(\bar{1}10)$	$(\bar{1}\bar{1}\bar{1})$	$(\bar{1}01)$	$(\bar{1}\bar{2}1)$
$(\bar{2}01)$	$(\bar{2}\bar{1}1)$	$(\bar{2}\bar{1}0)$	$(\bar{2}00)$				
			$(\bar{3}00)$				

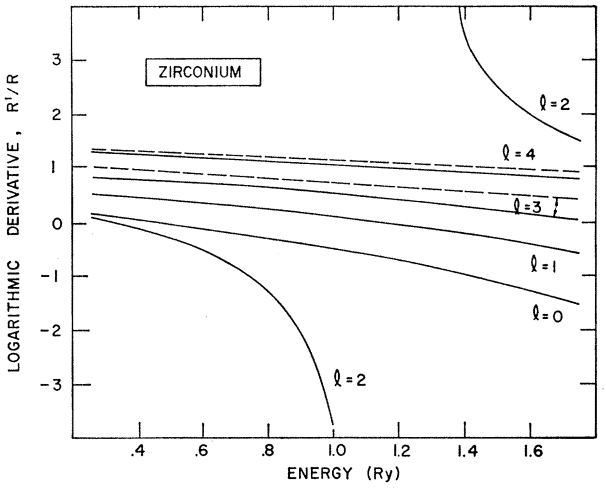

FIG. 1. Logarithmic derivatives (at APW sphere radius) as a function of energy. Dashed lines are results for zero potential.

reported by TJ. Some of the energy bands, however, were found to be very flat near the Fermi energy, and the Fermi surface is therefore very sensitive to the choice of potential. Slight modifications of the APW Fermi surface were therefore employed to bring it into closer agreement with the experimental results. Additional dHvA periods can be predicted from the APW Fermi surface, thus making further experimental results desirable as soon as better crystals of Zr become available.

DETAILS OF THE CALCULATION

The APW method has been discussed extensively in previous publications[7,8] and will not be reviewed in

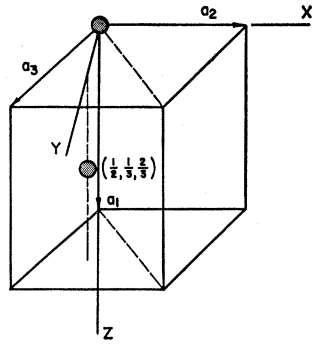

FIG. 2. Unit cell and half of the Brillouin zone for the hexagonal close-packed crystal structure.

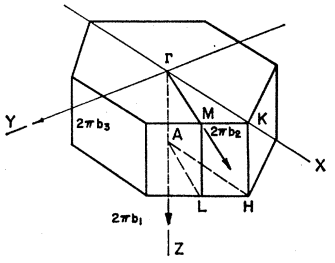

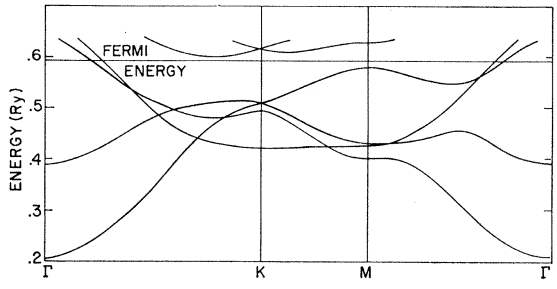

FIG. 3. Energy bands for zirconium along symmetry directions.

this article. Only the parameters used in this specific calculation will be summarized. The lattice constants[19] were taken to be $a=6.106$ and $c=9.728$ atomic units (a.u.).[20] The APW sphere radius were chosen to be $\exp(1.05)=2.858$. The muffin-tin potential was constructed according to the method suggested by Mattheiss[21]; the atomic Hartree-Fock-Slater self-consistent-field calculations of Liberman *et al.*[22] were used. Exchange was treated throughout in the Slater free-electron approximation. The muffin-tin potential is listed in Table I. The logarithmic derivatives (at the APW sphere radius) based on this potential are shown in Fig. 1.

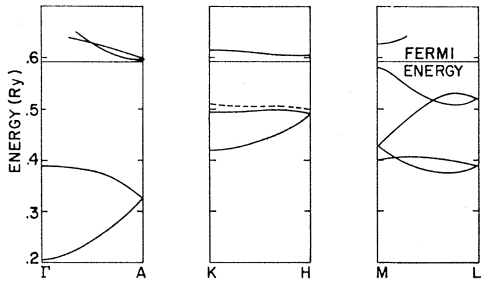

FIG. 4. Enery bands for zirconium along symmetry directions. The dashed curve along KH is orbitally doubly degenerate.

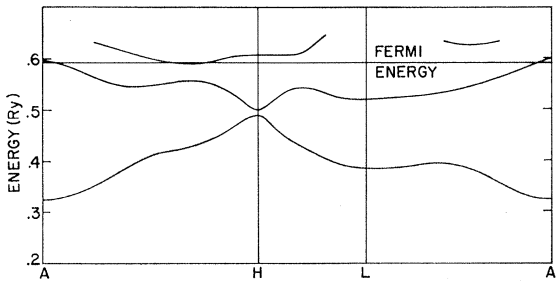

FIG. 5. Energy bands for zirconium along symmetry directions. All levels in this figure are orbitally doubly degenerate.

[19] R. W. G. Wyckoff, *Crystal Structures* (Interscience Publishers, Inc., New York, 1963), Vol. 1.

[20] Atomic units (a.u.) specified by $e^2=2$, $m=\frac{1}{2}$, and $h=2\pi$ are used throughout. The unit of length is the Bohr radius, and the unit of energy is the ionization potential of hydrogen (13.6 eV).

[21] L. F. Mattheiss, Phys. Rev. **134**, A970 (1964).

[22] D. Liberman, J. T. Waber, and Don T. Cromer, Phys. Rev. **137**, A27 (1965).

The unit cell and Brillouin zone for the hcp crystal structure are shown in Fig. 2. The basis vectors of the direct and reciprocal lattices are given by

$$\mathbf{a}_1=c\hat{k},\mathbf{a}_2=a\hat{\imath},\mathbf{a}_3=a(-\tfrac{1}{2}\hat{\imath}+\tfrac{1}{2}\sqrt{3}\hat{\jmath}),$$

and

$$\mathbf{b}_1=\hat{k}/c,\mathbf{b}_2=(\hat{\jmath}+\sqrt{3}\hat{\imath})/(a\sqrt{3}),\mathbf{b}_3=2\hat{\jmath}/(a\sqrt{3}).$$

The reciprocal lattice vectors,

$$\mathbf{g}=(n_1n_2n_3)=2\pi(n_1\mathbf{b}_1+n_2\mathbf{b}_2+n_3\mathbf{b}_3)$$

used in the APW expansion are listed in Table II. They were chosen on the basis of a convergence study of the energy levels (beneath the Fermi energy) at the points of high symmetry indicated in Fig. 2. They occur in the matrix elements in the form $\mathbf{k}+\mathbf{g}$, where $\mathbf{k}$ is the wave vector of the electronic state.

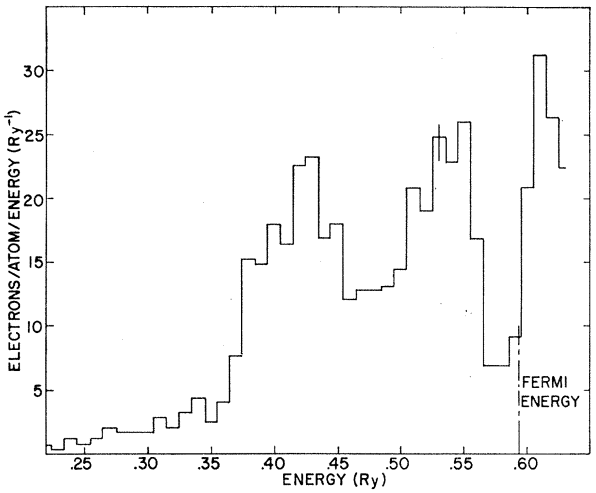

FIG. 6. Density-of-states curve for zirconium.

RESULTS

The energy bands along symmetry directions are shown in Figs. 3–5. Eigenvalues were also calculated at 250 general points in the 1/24 zone outlined by the points of high symmetry in Fig. 2. The location of these 250 points has been discussed in a previous article.[16] These eigenvalues were used to determine the Fermi energy (0.387 Ry relative to the bottom of the band) and the density-of-states curve shown in Fig. 6.

The principal pieces of the APW Fermi surface are shown in Figs. 7 and 8. The third- and fourth-zone hole surfaces are shown in Fig. 7 (double-zone scheme). These surfaces have (to within the accuracy of the calculation) cylindrical symmetry about the c axis and are centered on the ΓA edge of the Brillouin zone. The cross-sectional areas of the hole surfaces at points along this edge are shown in Fig. 9. The fifth-zone electron surface is shown in Fig. 8. It is centered at the symmetry point H. Cross sections of this surface

perpendicular to the c axis are shown in Fig. 10. A "side view" (perpendicular to the ΓAHK face) is shown in Fig. 11. The APW Fermi surface also has small ellipsoidal-shaped pieces of the Fermi surface in the sixth zone. These electron surfaces are shown in Fig. 11; they are inside the "pillars" of the fifth-zone electron surface, contacting it along the AHL plane.

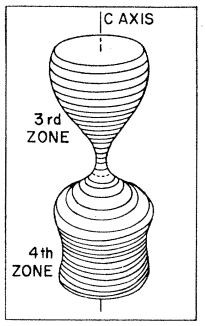

FIG. 7. Third- and fourth-zone holes of the APW Fermi surface for zirconium (double-zone scheme).

DISCUSSION

The APW Fermi surface is almost entirely different from the model of AB.[2] It is interesting to point out the modifications in our energy bands which would be necessary to reproduce their results. In Fig. 3, for instance, we see that the fifth band is always above the Fermi energy. They found that this band dipped below the Fermi energy from about $0.6\Gamma K$–$0.9\Gamma K$ and from about $0.4\Gamma M$–$0.5\Gamma M$. Furthermore, they found the fourth band to be above the Fermi energy in the vicinity of the symmetry point M. This feature would also occur in Fig. 4 where, in addition, their third band dips below the Fermi energy near A. In Fig. 5 they found the fifth and sixth bands to intersect the Fermi energy closer to A than to H, and these bands also

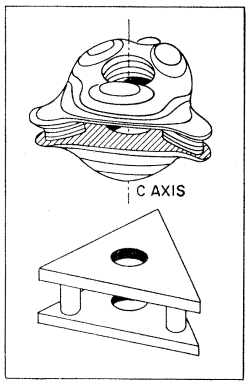

FIG. 8. Fifth-zone electrons of the APW Fermi surface for zirconium (upper) with a schematic diagram (lower) intended to aid in visualizing this complicated surface.

dipped below the Fermi energy from about $0.3AL$–$0.5AL$. They also found the third and fourth bands to be above the Fermi energy in the vicinity of the symmetry point L. In Figs. 4 and 5 we find these levels to be substantially below the Fermi energy near L.

It thus appears from this comparison of our results with those of AB that although the Fermi surfaces are almost entirely different, it is possible to modify the energy bands and make them similar. Some of these modifications are justifiable because the potentials used in both calculations were not self-consistent. With an *ad hoc* potential it is not reasonable to state, for instance, whether or not the third band drops below the Fermi energy near the symmetry point A. A measure of the dependence of the energy bands on the potential can be found by examining other calculations for hcp transition metals. For instance, we can look at the energy bands of Re[12] near the Fermi energy corresponding to four electrons per atom (the case for Zr). We find that the upper doubly-degenerate level at A in Fig. 4 is about 0.01 Ry *below* the Fermi energy. Furthermore, just as was found by AB, the fourth band is above the Fermi energy at the symmetry point M. On the other hand, the position of the crossing of the fifth and sixth bands along AH, the location of the third and fourth bands at L, and the location of the fifth and sixth bands along AL are all qualitatively the same for Re (in this rigid-band approximation) and the APW calculation for Zr. We can also compare results with the energy bands for Dy,[17] which are also quite similar to those for

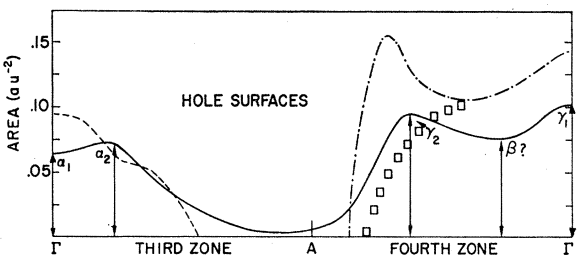

FIG. 9. Cross-sectional area of the third- and fourth-zone hole surfaces. Solid line is the APW Fermi surface. The broken lines and the squares indicate possible modifications of the Fermi surface which are discussed in the text.

Y. In this case we find a close agreement with the present results for Zr except that in Fig. 5 the fifth and sixth bands cross the Fermi energy at H instead of along AH.

We conclude from the above comparisons that the details of the energy bands (and hence the Fermi surface) are extremely sensitive to the potential. Hence, it is not surprising that our results differ substantially from those of AB whose potential was based on atomic self-consistent-field calculations for Zr^{4+} and the uniform charge distribution of three electrons per atom, consideraly different from the potential used in our APW calculation.[8] As a corollary, we accept the fact that since a self-consistent crystal potential was not used in either case, then neither of the calculations should be accepted without considerable caution.

Nevertheless, it turns out that our Fermi-surface model can qualitatively account for all of the dHvA periods observed by TJ and seems to be a good model from which to begin an interpretation of their data. In the following paragraphs we describe the model and

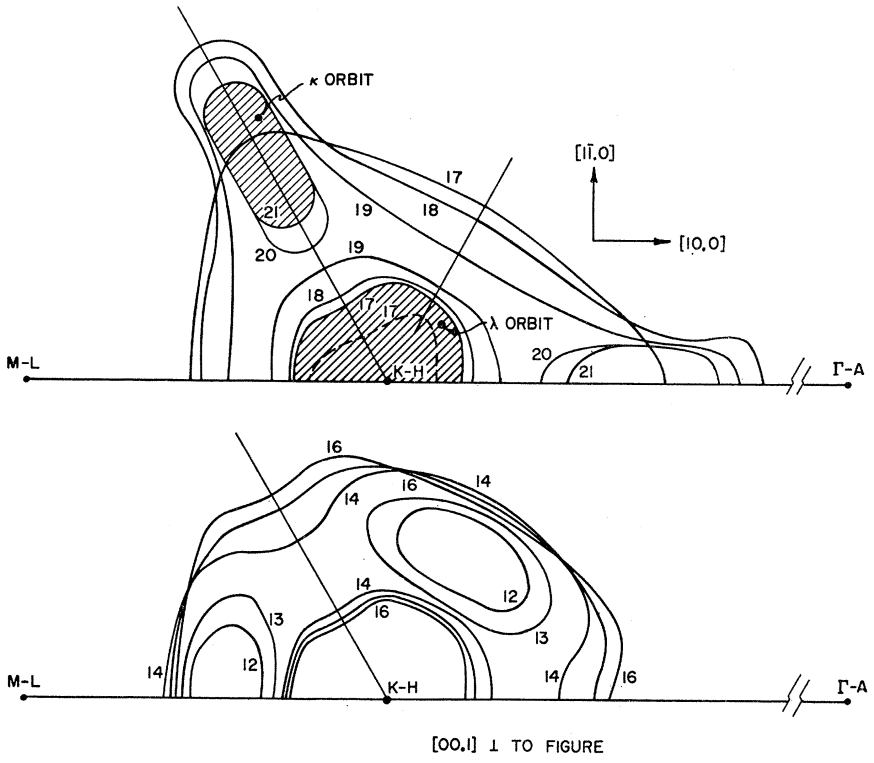

FIG. 10. Cross sections of the fifth-zone electron surface perpendicular to the c axis. The KH edge was divided into twenty equal increments, and the numbers refer to the corresponding planes (21 is the AHL plane). The dotted line (17) indicates a possible modification of the APW Fermi surface.

its relationship with the experimental results, suggesting in some instances how the APW Fermi surface can be modified to make it more consistent with the observed data.

The easiest pieces of the Fermi surface to discuss are the third- and fourth-zone holes shown in Fig. 7. The areas of cross sections normal to the c axis are given in Fig. 9. The dHvA periods based on this surface are given in Fig. 12. They have many of the characteristics of the α, β, and γ periods observed by TJ,[1] but differ in certain details. By modifying the APW Fermi surface slightly the more objectionable differences can be eliminated. For instance, it is tempting to associate the upper period in Fig. 12 with the α orbit, but the experimental results indicate that this corresponds to a closed surface of nearly constant cross-sectional area. By pulling the upper doubly-degenerate level at A (Fig. 4) below the Fermi energy, the neck on the third- and

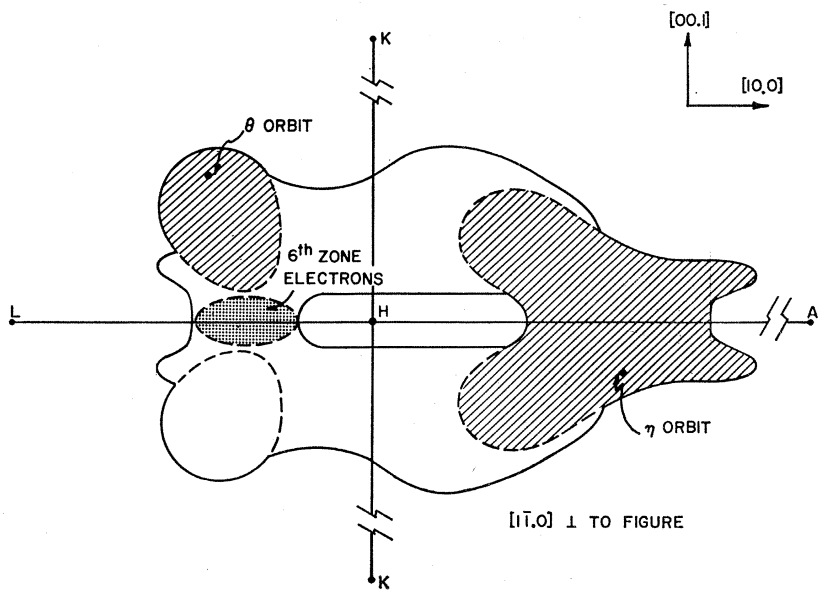

FIG. 11. View of the fifth-zone electron surface perpendicular to the ΓAHK face ($\perp$ to the [1$\bar{1}$.0] direction).

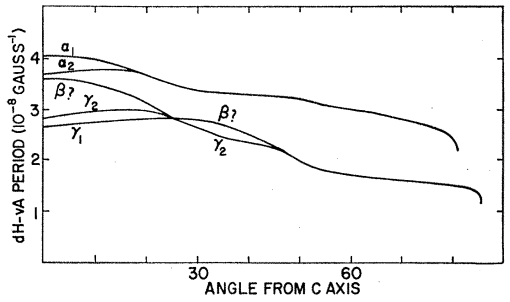

FIG. 12. de Haas–van Alphen periods calculated from the third- and fourth-band holes of the APW Fermi surface (Fig. 9). Results based on the modified Fermi surface are shown in Fig. 13.

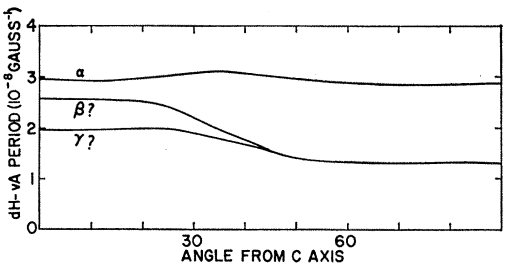

FIG. 13. de Haas–van Alphen periods calculated from the modified Fermi surface shown in Fig. 13. Results based on the APW Fermi surface are shown in Fig. 12.

fourth-zone holes is broken, as shown by the dashed and broken lines in Fig. 9. The dHvA periods based on this modified version of the Fermi surface are shown in Fig. 13. We have adjusted the size and shape of the modified third-zone hole surface to give reasonable agreement with the experimental results. Since the modifications do not require very drastic alterations of the APW results, we conclude that the α orbit is associated with the third-band holes at Γ.

The other two dHvA periods in Fig. 13 are based on the modified fourth-zone holes shown by the broken line in Fig. 9. The modifications were designed to bring these two curves into approximate agreement (for angles less than 30°) with the β and γ periods of TJ. Although this was possible, it resulted in a considerable increase in the volume contained by this piece of surface. The modifications required on the third-zone surface, on the other hand, were such that the volume remained nearly constant. Thus it is tempting to consider a less severe modification such as the one indicated by the squares in Fig. 9. This would yield the γ period (indicated with a question mark) in Fig. 13, but would eliminate the β period. We cannot definitely say that either of these two possible surfaces accounts for the β and/or γ orbits. They are presented merely as possible interpretations. Both of these modified fourth-zone surfaces are closed and should support dHvA periods at all angles. In order for this orbit assignment to be correct there must be another factor (such as heavy effective mass) which precludes these orbits from being observed for angles greater than about 30°.

The β orbit (and possibly γ also) can also be assigned to an extremal orbit on the fifth-zone electron surface shown in Fig. 8. This surface is multiply connected and can also account for the remaining dHvA periods designated ϵ and δ by TJ. In Fig. 14 we have indicated the corresponding extremal orbits. The δ period, for instance, was observed only in a limited angular range for field directions near [10.0]. The corresponding orbit is indicated in Fig. 14. In order to describe this orbit (and others which follow) it is necessary to agree on some terminology.

Looking at Fig. 8 we notice that the fifth-zone electron surface has six protuberances which resemble "duck beaks." Pairs of these are separated vertically

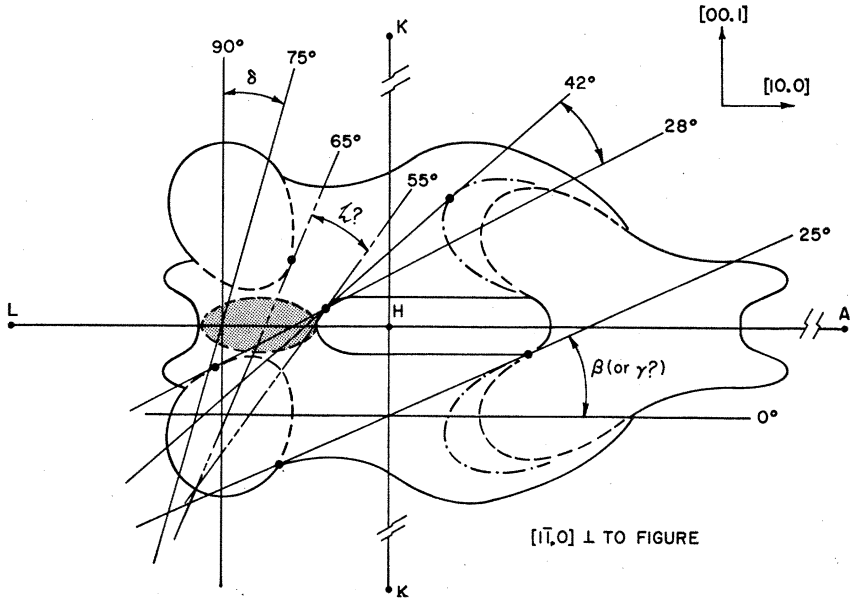

FIG. 14. View of the fifth-zone electron surface perpendicular to the ΓAKH face ($\perp$ to $[1\bar{1}.0]$ direction) showing edges of planes which intersect the surface at extremal cross sections. Angles correspond to field directions in the $(1\bar{1}.0)$ plane measured from the [00.1] direction. The dot-dashed line indicates a modification of the Fermi surface which makes it more consistent with the experimental results.

(with reference to the orientation of the drawing) by "pillars" with ellipsoidal cross sections. Horizontally these "beaks" are connected by the "arms" of torus-like shapes. We will distinguish between these two torus shapes by arbitrarily calling one "upper" and the other "lower."

The δ orbit in Fig. 14 runs along the outer sides of two vertically opposed "arms" and closes on the outer sides of the two adjacent "pillars." In our model this orbit is an extremal for field directions in the range 0–15° from [10.0]. About 15° away from [10.0] toward [00.1] the orbit falls off the "arms," and 15° away from [10.0] toward [1$\bar{1}$.0] it can no longer remain on both of the "pillars." The dHvA period calculated from our Fermi surface for this orbit is 2.3×10^{-8} G^{-1} compared to the experimental value 3.3×10^{-8} G^{-1}, the area of the electron surface being too large by a factor of about 1.4. We will see that this same factor applies to the other orbits on this piece of surface.

The ϵ orbit is also indicated in Fig. 14. It goes along the side of one of the lower "arms", up the two adjacent "pillars" and over onto the two opposing upper "arms." The discontinuity between the ϵ and δ orbits is due to the hole in the torus-like portion of the surface. The dot-dashed line is a possible modification of the APW surface which makes it more consistent with the observed angular dependence of the dHvA periods. We find an approximate value for the dHvA period to be 2.0×10^{-8} G^{-1} compared with experimental results ranging from 2.7–2.9×10^{-8} G^{-1}, the theoretical surface again being too large by a factor of about 1.4.

As indicated in Fig. 14 there is also an extremal orbit around the outside of the torus-like portion of the electron surface. This orbit has the proper angular dependence to be assigned to either the β or γ periods of TJ. (As mentioned earlier, these might also be associated with the fourth-zone hole surface.) The dHvA period calculated from the electron surface is about 2.0×10^{-8} G^{-1} compared to the experimental result 2.7×10^{-8} G^{-1} for the β period. Since this indicates a theoretical surface which is too large by a factor of about 1.4 (just as was found for the δ and ϵ orbits), we have decided to assign this orbit to the β period.[23] This leaves the γ period to be associated with the fourth-zone hole surface.

If the modified Fermi surface we have presented is qualitatively correct, then there are other dHvA periods which should be observed. The continuation of the γ period past about 30° as indicated in Fig. 13 is the only one of these which is inconsistent with the published data. All the other periods are much larger than those reported by TJ and conceivably will be observed whenever better crystals become available. For instance, there is an orbit designated ζ in Fig. 14 which should occur in the angular range between ϵ and δ, i.e., about 55°–65° from [00.1] to [10.0]. It goes along the outside of one of the lower "arms," up the outside of the two adjacent "pillars," over the two opposed upper "arms" and *back down* the inside of the same two adjacent "pillars." The period is estimated to be about 5.0×10^{-8} G^{-1}. Of the new orbits, however, it is the least likely to be observed since it depends critically on the topography of the Fermi surface.

In addition, there are two new orbits which should be observed for field directions around the [00.1] direction. These are indicated in Fig. 10. The κ orbit is around the "pillars" and the λ orbit is inside the torus-like rings. The λ orbit should correspond to a dHvA period of about 11×10^{-8} G^{-1}. If the hole is smaller (see dotted line in Fig. 10), as was required in Fig. 14 in order to give the correct angular dependence for the ϵ orbit, the period could be as much as twice this estimated value. The κ orbit is much smaller and should yield a dHvA period of about 30×10^{-8} G^{-1}.[24]

Two other new orbits are indicated in Fig. 11. The θ orbit is around the "arms" and should have a period of about 20×10^{-8} G^{-1} with the field in the [1$\bar{1}$.0] direction.[25] The η orbit should have a period of about 5.5×10^{-8} G^{-1} for this field orientation.

We conclude this discussion with a few remarks on the density-of-states curve (Fig. 6). It has the same general shape as has been found in other APW calculations for hcp transition elements.[12–17] The Fermi energy occurs slightly on the high-energy side of a sharp minimum in the density-of-states curve. Neighboring yttrium, on the other hand, has a Fermi energy near the top of the peak on the low energy side of this minimum. This is indicated by a small vertical line in Fig. 6. We would expect, therefore, that the electronic specific-heat coefficient for Zr would be smaller than for yttrium. The ratio of their experimental values[26,27] (Y/Zr) is about 3.6. The ratio of their theoretical values[17] (using 3.8×10^{-4} cal/mole deg^2 calculated from Fig. 6) is about 3.0, which is reasonable since we have not considered different electron-phonon enhancement factors. The ratio of the experimental to the theoretical result for Zr indicates an electron-phonon enhancement factor of about 1.8, consistent in magnitude with results found for other transition metals.

CONCLUSIONS

The above discussion is lengthy and probably would be clarified by a few summarizing remarks. The third-

[23] There is a small discontinuity in the experimental β period about 15° from [00.1] to [10.0]. It is possible that this is due to scatter in the data; it should at least be mentioned, however, that at about this same angle the β orbit on the electron surface jumps up over one of the "duck beaks" (see right-hand side of Fig. 14), thus creating a discontinuity in the extremal cross sections.

[24] The sixth-zone electrons form little ellipsoidal pockets inside the pillars on the fifth-zone surface. Their maximum cross section should be about the same as the κ orbit, corresponding to a minimum period of about 30×10^{-8} G^{-1}.

[25] For certain field orientations the θ orbit can move off the large central portion of the "arms" toward the "pillars" at each end.

[26] H. Montgomery and G. P. Pells, Proc. Phys. Soc. (London) **78**, 622 (1961).

[27] G. D. Kneip, Jr., J. O. Batteton, Jr., and J. O. Scarbrough, Phys. Rev. **130**, 1687 (1963).

zone electron surface is centered at Γ and has a nearly uniform extremal cross section (see the modified surface in Fig. 9) which we associate with the α period of TJ. Their γ period corresponds to the central extremal orbit of the fourth-zone hole surface which is also shown in Fig. 9. Possible shapes of this hole surface are indicated by both the broken line and the line of squares in Fig. 9. It is not possible to distinguish between these surfaces because the experimental dHvA periods are not observed beyond about 30° from the [00.1] direction.

The β, δ, and ϵ periods are associated with the multiply connected fifth-zone electron surface centered at H. The areas of the extremal orbits based on the APW surface are consistently too large by a factor of about 1.4, but have approximately the correct angular dependence. The sixth-zone electrons are very small pieces which have not been observed experimentally.

ACKNOWLEDGMENT

Many of the details of the calculations reported here were very diligently carried out by Ken Moseley.

PHYSICAL REVIEW VOLUME 159, NUMBER 3 15 JULY 1967

Damping of Phonons in Aluminum

G. Björkman, B. I. Lundqvist, and A. Sjölander
Institute of Theoretical Physics, Göteborg, Sweden
(Received 17 January 1967)

The damping of phonons in Al due to the electron-phonon interaction has been calculated using an effective ion-electron interaction potential given recently by Vosko *et al.* The results show that this effect is essential, although not sufficient, to account for the experimental data of Nilsson and Stedman.

I. INTRODUCTION

Recently, very precise measurements of the phonon dispersion curves for Al at 80°K were reported by Nilsson and Stedman.[1] The lifetimes of the individual phonons were also measured. In order to explain the significantly larger damping of the longitudinal phonons compared with the transverse phonons, Nilsson and Stedman conjectured that at these low temperatures the major part of the damping of the phonons arises from electron-phonon interaction and to a lesser extent from anharmonic effects. Several authors have given order-of-magnitude estimates of the phonon lifetimes arising from electron-phonon interaction[2,3] as well as anharmonicity,[3,4] but to our knowledge no quantitative calculations of the lifetimes in Al have been reported. On the other hand, several calculations of the phonons dispersion curves have been carried out, based on pseudopotential methods.[5,6]

We have taken advantage of this in our calculations by using the same pseudopotential as given by Vosko *et al.*[6] in their calculations of the phonon dispersion curves in Al, which shows quite good agreement with the experimental results.[1] Our aim has been to carry out a sufficiently accurate calculation of the phonon lifetimes as a function of the phonon wave vector and compare with the experimental data in order to ascertain whether the electron-phonon coupling gives the main contribution or not.

II. THEORY

Our calculations are essentially a repetition of earlier calculations by Woll and Kohn,[7] but with a more realistic effective ion-electron interaction.

The basic quantity entering into the theory of lattice vibrations is the dynamical matrix, which can be written in the following form[8]:

$$\mathbf{D}(\mathbf{q})=\frac{1}{Mv_a}\sum_{\mathbf{K}}[(\mathbf{q}+\mathbf{K})(\mathbf{q}+\mathbf{K})v_{\mathrm{eff}}(\mathbf{q}+\mathbf{K}) - \mathbf{K}\mathbf{K}v_{\mathrm{eff}}(\mathbf{K})], \quad (1)$$

[1] R. Stedman and G. Nilsson, Phys. Rev. **145**, 492 (1966).
[2] J. J. J. Kokkedee, Physica **28**, 893 (1962); J. J. J. Kokkedee, in *Proceedings of the Conference on Inelastic Scattering of Neutrons in Solids and Liquids* (International Atomic Energy Agency, Vienna, 1963), Vol. I, p. 15. M. A. Krivoglaz, Fiz. Tverd. Tela **3**, 2761 (1963) [English transl.: Soviet Phys.—Solid State **3**, 2015 (1962)].
[3] R. J. Elliott and H. Stern, in *Proceedings of the Conference on Inelastic Scattering of Neutrons in Solids and Liquids* (International Atomic Energy Agency, Vienna, 1961), p. 61.
[4] J. J. J. Kokkedee, Physica **28**, 374 (1962); A. A. Maradudin and A. E. Fein, Phys. Rev. **128**, 2589 (1962).
[5] W. A. Harrison, *Pseudopotentials in the Theory of Metals* (W. A. Benjamin, Inc., New York, 1966); W. A. Harrison, Phys. Rev. **129**, 2522 (1963).
[6] S. H. Vosko, R. Taylor, and G. H. Keech, Can. J. Phys. **43**, 1187 (1965).
[7] E. J. Woll and W. Kohn, Phys. Rev. **126**, 1693 (1962). A factor $\frac{1}{2}$ seems to be missing in their Eq. (4.4). It should be noted that their expression for $1/\tau$ refers to the damping rate of the phonon energy and thus by definition corresponds to $2/\tau$ in our notation.
[8] See, for instance, A. Sjölander, in *Symposium on Inelastic Scattering of Neutrons by Condensed Systems*, edited by L. M. Corliss (BNL, Upton, New York, 1966), p. 29.